

Journal of Materials Chemistry C

Accepted Manuscript



This is an *Accepted Manuscript*, which has been through the Royal Society of Chemistry peer review process and has been accepted for publication.

Accepted Manuscripts are published online shortly after acceptance, before technical editing, formatting and proof reading. Using this free service, authors can make their results available to the community, in citable form, before we publish the edited article. We will replace this *Accepted Manuscript* with the edited and formatted *Advance Article* as soon as it is available.

You can find more information about *Accepted Manuscripts* in the [Information for Authors](#).

Please note that technical editing may introduce minor changes to the text and/or graphics, which may alter content. The journal's standard [Terms & Conditions](#) and the [Ethical guidelines](#) still apply. In no event shall the Royal Society of Chemistry be held responsible for any errors or omissions in this *Accepted Manuscript* or any consequences arising from the use of any information it contains.



ARTICLE

Synthesis of novel nonlinear optical chromophores: achieving excellent electro-optic activity by introducing benzene derivative isolation groups into the bridge

Received 00th January 20xx,
Accepted 00th January 20xx

DOI: 10.1039/x0xx00000x

www.rsc.org/

Chaolei Hu,^{ab} Fenggang Liu,^{ab} Hua Zhang,^{ab} Fuyang Huo,^{ab} Yuhui Yang,^{ab} Haoran Wang,^{ab} Hongyan Xiao,^a Zhuo Chen,^a Jialei Liu,^a Ling Qiu,^a Zhen Zhen,^a Xinhou Liu^a and Shuhui Bo^{a*}

Three novel second order nonlinear optical (NLO) chromophores based on julolidinyl donors and tricyanofuran (TCF) acceptors linked together via modified polyene π -conjugation with rigid benzene derivative steric hindrance groups (chromophores CL1 and CL2) or unmodified polyene π -conjugation (chromophores CL) moieties as the bridges have been synthesized in good overall yields and systematically characterized. Density functional theory (DFT) was used to calculate the HOMO–LUMO energy gaps and first-order hyperpolarizability (β) of these chromophores. Besides, to determine the redox properties of these chromophores, cyclic voltammetry (CV) experiments were performed. Compared with CL, after introducing benzene derivative steric hindrance groups into the bridge, chromophores CL1 and CL2 had good thermal stabilities with high thermal decomposition temperatures which were 32°C, 24°C higher than chromophore CL, respectively. Most importantly, the introduction of rigid steric hindrance groups can effectively reduce dipole–dipole interactions to translate their relatively small β values into bulk high EO activities. By doping chromophores CL, CL1 and CL2 with a high loading of 45 wt % in APC, EO coefficients (r_{33}) of up to 121, 197 and 202 pm V⁻¹ at 1310 nm can be achieved, respectively. The r_{33} values of new chromophores CL1 and CL2 were about 1.6 times of chromophore CL. The high r_{33} value, good thermal stability and high yield suggest the potential use of the new chromophores in nonlinear optical area.

Introduction

Organic and polymeric electro-optic (EO) materials have been intensively studied for several decades due to their potential applications for the information technologies, THz generation/detection systems, integrated circuits and multifunctional nanodevices.^{1–6} These potential applications have stimulated a research boom for materials with large EO activities, both at the molecular level (β) and as processed materials (r_{33}).⁷ The type of poled guest–host polymeric material in which an EO chromophore is dispersed in a polymer matrix, is the most highly studied materials in this field.⁸ However, for practical applications, EO materials require large nonlinear coefficients (r_{33} values) and strong thermal and photochemical stability.⁹ Thus, optimizing chromophores with large r_{33} values and good stability simultaneously has become the focus of the researchers.

Second-order NLO chromophores are based on a push–pull

system, which consists of an electron-donating group (donor) and an electron-withdrawing group (acceptor) coupled through a π -conjugated bridge.^{10,11} In order to achieve large EO activities, many efforts have been carried out to design and synthesize novel NLO chromophores, seeking to engineer NLO molecules both microscopically (β) and macroscopically (r_{33}). The majority of these works were aiming at introducing long chain isolation groups (IGs) to the donor or bridge, which can improve the solubility and suppress the dipole interactions among chromophores.^{7, 12–21} However, the effect of the long chain is not good, and the macroscopic NLO activity (r_{33}) enhanced less. So far, the research of introducing a rigid IG into the bridge is rare. As we all know, the benzene ring is a rigid structure, and has good stability. Besides, some benzene derivatives such N,N-dimethylaniline have the advantages of good electron-donating ability and good solubility. Based on the above, modifying π -conjugated bridge by introducing a rigid IG into the π -conjugated bridge may be a useful method to improve the EO activity, stability and solubility.

In this article, the motivation is to improve the EO activities of guest-host EO materials by a simple modification of π -electron bridges for NLO chromophores. Adding the suitable IGs to the conjugated electronic bridge was carried out to facilitate the chromophores with different steric hindrance and free mobility, which was expected to achieve the large macroscopic EO

a Key Laboratory of Photochemical Conversion and Optoelectronic Materials, Technical Institute of Physics and Chemistry, Chinese Academy of Sciences, Beijing 100190, PR China. E-mail: boshuhui@mail.ipc.ac.cn; Fax: +86-01-82543530; Tel: +86-01-82543529

b University of Chinese Academy of Sciences, Beijing 100043, PR China
DOI: 10.1039/x0xx00000x

coefficients by optimizing the poling condition in guest-host EO polymers.⁷ Due to their high electron-density and low cost, methoxyphenyl unit and N,N-dimethylaniline unit especially the latter have been widely studied in the dye-sensitized solar cells (DSCs).^{10, 22, 23} In this work, benzene derivative steric hindrance groups, methoxyphenyl unit and N,N-dimethylaniline unit, were chosen to introduce into the polyene π -electron bridges. These two steric hindrance groups can act as both the additional donor (electron effect) and the isolation groups (steric effect). The position of the IG is very important to the EO activity for chromophores, and benzene derivative steric hindrance groups were arranged on the bridge and opposite to the long chain of the donors. This structure is an effective approach to suppress the dipole interactions among chromophores and improve the poling efficiency, thus achieving much larger macroscopic NLO activity.

Based on the above, we had designed and synthesized chromophores CL1 and CL2 by modifying π -electron bridges. Chromophore CL containing no steric hindrance group on the π -bridge had been synthesized for comparison. The synthesis, UV-vis, solvatochromic, density functional theory (DFT) quantum mechanical calculation, redox property, thermal stability and EO activity of these chromophores were systematically studied and compared to illustrate the architectural influences on rational NLO chromophore designs (Chart 1). By doping novel chromophores CL1 and CL2 with a high loading of 45 wt % in APC, EO coefficients (r_{33}) of up to 197 and 202 pm V⁻¹ at 1310 nm can be achieved, respectively.

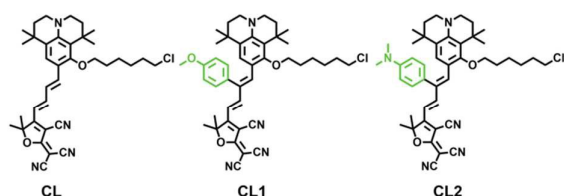


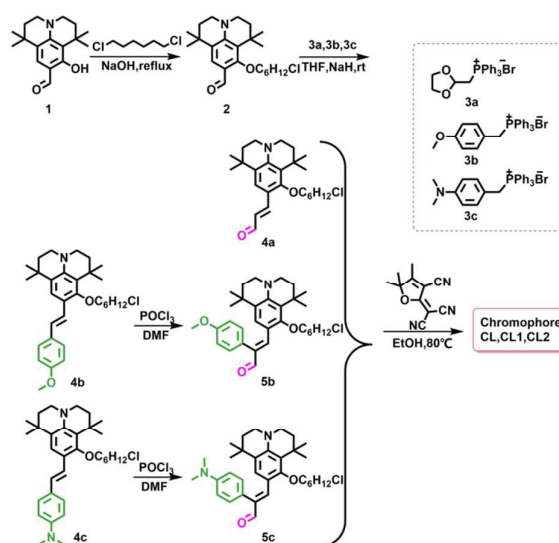
Chart 1 Chemical structure for chromophores CL, CL1 and CL2.

Results and discussion

Synthesis and characterization of chromophores

Chromophores CL, CL1 and CL2 were synthesized following the general route laid out in Scheme 1. Starting from 8-hydroxy-1,1,7,7-tetramethyljulolidine-9-carboxaldehyde, chromophores CL, CL1 and CL2 were synthesized in good overall yields (40%~50%) through simple three or four step reactions: The derivative **2** was obtained by substituting of **1** with 1,6-dichlorohexane. After introduction of

the bridge by Wittig condensation, compounds **4a–c** were prepared with a high yield. Treatment of compounds **4b–c** with POCl₃ and DMF gave aldehydes **5b–c**. And the final condensations with the TCF acceptor give chromophores CL, CL1 and CL2 as green solids. All the chromophores were completely characterized by ¹H NMR, ¹³C NMR, MS, UV-Vis spectroscopic analysis and the data obtained were in full agreement with the proposed formulations. These chromophores possess good solubility in common organic solvents, such as dichloromethane, chloromethane and acetone.



Scheme 1 Chemical structures and synthetic routes for chromophores CL, CL1 and CL2.

Thermal stability

NLO chromophores must be thermally stable enough to withstand high temperatures (>200°C) in electric field poling and subsequent processing of chromophore/polymer materials. Chromophore CL1 has the highest decomposition temperature (273 °C), followed by CL2 (265 °C) and CL (241°C) as shown in Table 1 and Fig. 1. Chromophores CL1 and CL2 had a much higher decomposition temperature than chromophore CL with no steric hindrance on the π -electron bridge. The enhanced thermal stability of chromophores CL1 and CL2 over chromophore CL is due to the introduction of benzene derivative steric hindrance groups into π -electron bridges. While chromophores CL1 and CL2 had a similar steric hindrance on the π -electron bridge, they show different decomposition temperatures of 273 °C and 265 °C, respectively.

Table 1 Summary of thermal and optical properties and EO coefficients of chromophores CL, CL1 and CL2

Chromophores	T_d^a (°C)	λ_{max}^b (nm)	λ_{max}^c (nm)	$\Delta\lambda^d$ (nm)	r_{33}^e (pm V ⁻¹)
CL	241	709	624	85	121
CL1	273	703	627	76	197
CL2	265	706	633	73	202

^a T_d was determined by an onset point and measured by TGA under nitrogen at a heating rate of 10 °C min⁻¹. ^b λ_{max} was measured in chloroform. ^c λ_{max} was measured in dioxane. ^d $\Delta\lambda = \lambda_{max}^b - \lambda_{max}^c$. ^e r_{33} values were measured at the wavelength of 1310 nm.

This may be attributed to the different properties of groups ($-\text{OCH}_3$, $-\text{N}(\text{CH}_3)_2$). The excellent thermal stability of these chromophores makes them suitable for practical device fabrication and EO device preparation.

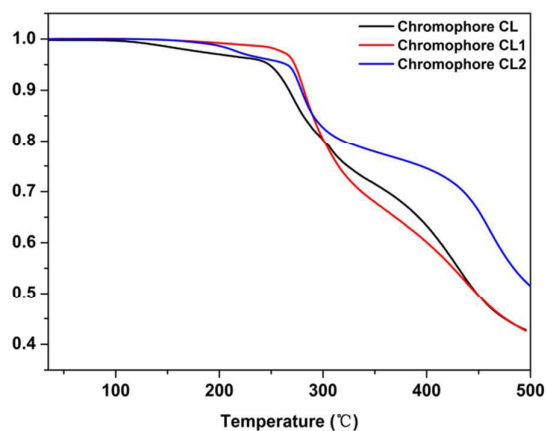


Fig. 1 TGA curves of chromophores CL, CL1 and CL2 with a heating rate of $10^\circ\text{C min}^{-1}$ in a nitrogen atmosphere

Optical properties

In order to reveal the effect of different steric hindrance group on the intramolecular charge-transfer (ICT) of dipolar chromophores, UV-Vis absorption spectra of the three chromophores ($c = 1 \times 10^{-5} \text{ mol L}^{-1}$) were measured in a series of solvents with different dielectric constants as shown in Fig. 2. The spectral data are summarized in Table 1. Depending on different structures, the synthesized NLO chromophores exhibited a similar $\pi \rightarrow \pi^*$ intramolecular charge-transfer (ICT) absorption band in the visible region. As shown in Fig. 2, chromophore CL, CL1 and CL2 exhibited the maximum absorption (λ_{max}) from 703 nm to 709 nm in chloroform. The λ_{max} of chromophores CL1 and CL2 is similar with chromophore CL, which may attribute to the fact that the additional aromatic ring steric hindrance groups didn't change the conjugate structure. Moreover, it was accompanied by the change of absorption intensity for these three chromophores. As shown in Fig. 2, chromophore CL1 and CL2 showed more intensified intramolecular charge-transfer than chromophore CL. After comparing, it could be found that introduction of benzene derivative steric hindrance groups effectively enhanced the intensity of intramolecular charge-transfer.

Besides, the solvatochromic behavior was also explored to investigate the polarity of chromophores. It was found that all of the three chromophores showed very large bathochromic shifts of 85 nm, 76 nm and 73 nm respectively, when solvent was changed from dioxane to chloroform, displaying larger solvatochromism than that of CLD (60 nm)²⁴ and a similar single donor FTC (61 nm)²⁵ chromophore. It indicated that all of chromophores CL, CL1 and CL2 are more polarizable than the traditional chromophore FTC.

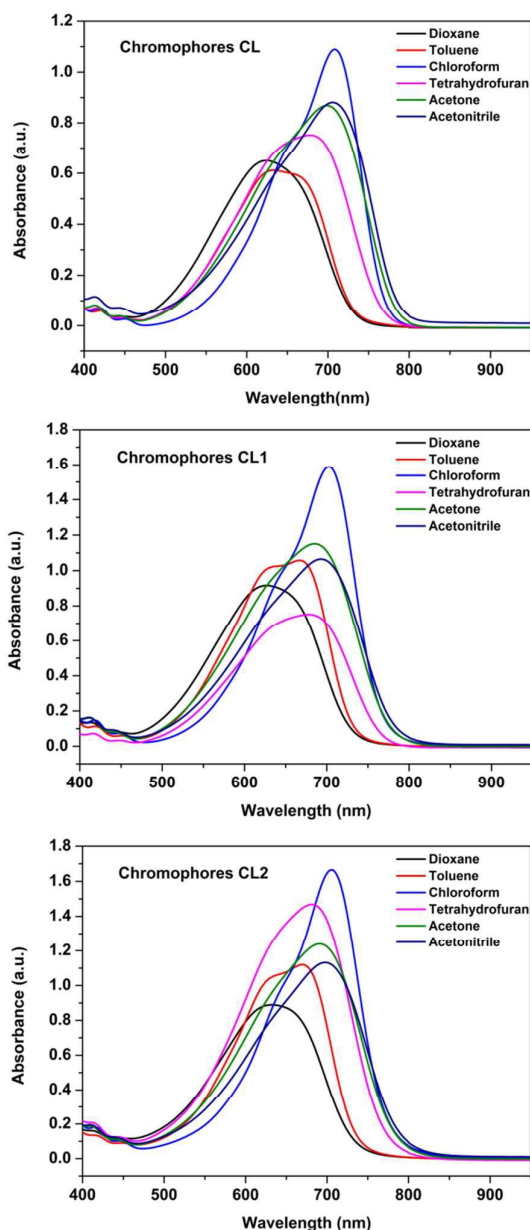


Fig. 2 UV-Vis absorption spectra of chromophores CL, CL1 and CL2 in six kinds of aprotic solvents with varying dielectric constants (ϵ)

Theoretical calculations

In order to model the ground state molecular geometries, the HOMO-LUMO energy gaps and β values of these chromophores were calculated. The DFT calculations were carried out at the hybrid B3LYP level by employing the split valence 6-31G* basis set.²⁶ The data obtained from DFT calculations are summarized in Table 2.

The HOMO and LUMO energies were calculated by DFT calculations as shown in Table 2. The energy gaps between the HOMO and LUMO energies for chromophores CL, CL1 and CL2 were 2.35 eV, 2.36 eV and 2.33 eV respectively. The HOMO-LUMO gap of

chromophore CL2 (2.33 eV) is lower than that of chromophore CL1 (2.36 eV). This may result from the fact that N,N-dimethylaniline has a stronger electron-donating ability than methoxyphenyl. The HOMO–LUMO gap of chromophore CL1 was little larger than chromophore CL, this may be explained by that conjugate structure was somehow wrecked by the lateral group methoxyphenyl. These results correspond to the UV-Vis results.

The frontier molecular orbitals are often used to characterize the chemical reactivity and kinetic stability of a molecule and to obtain

qualitative information about the optical and electrical properties of molecules. Besides, the HOMO–LUMO energy gap is also used to understand the charge transfer interaction occurring in a chromophore molecule. In the case of these chromophores, Fig. 3 represents the frontier molecular orbitals of chromophores CL, CL1 and CL2. According to Fig. 3, it is clear that, the electron density is concentrated on the donor moiety when at the HOMO state, while on the π -bridge and acceptor moiety when at the LUMO state.

Table 2 Electrochemical^a and DFT calculated^b properties of chromophores CL, CL1 and CL2

Cyclic voltammetry ^a				DFT calculations ^b					
Chromophores	E _{ox} /V	E _{red} /V	ΔE /eV	HOMO/eV	LUMO/eV	E _{ge} /eV	μ /D	$\beta/(10^{-30}\text{esu})$	
CL	0.23	-1.06	1.29	-5.26	-2.91	2.35	22.05	328.04	
CL1	0.19	-1.14	1.33	-5.22	-2.86	2.36	22.35	303.49	
CL2	0.10	-1.15	1.25	-5.14	-2.81	2.33	23.32	307.08	

^a 10^{-3} M in CH₃CN versus Ag/AgCl, glassy carbon working electrode, Pt counter electrode, 20 °C, 0.1M Bu₄NPF₆, 100mV s⁻¹ scan rate, ferrocene internal reference E_{1/2} = +0.43V. ^b DFT calculations at the B3LYP/6-31G* level in vacuum.

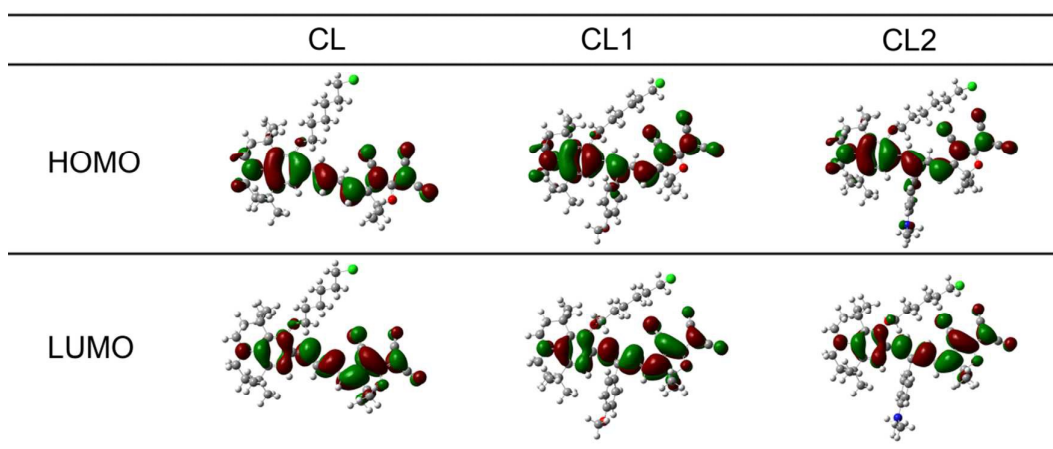


Fig. 3 The frontier molecular orbitals of chromophores CL, CL1 and CL2.

Table 3 The molecular orbital composition (%) in the ground state for chromophores CL, CL1 and CL2^a

Chromophore	CL		CL1		CL2	
	HOMO	LUMO	HOMO	LUMO	HOMO	LUMO
Donor	56.22%	38.03%	56.75%	36.26%	55.59%	36.21%
π -Bridge	9.96%	16.26%	10.19%	16.56%	10.07%	16.62%
Acceptor	33.82%	45.72%	30.48%	46.41%	30.25%	46.67%
Methoxyphenyl			2.57%	0.77%		
N,N-dimethylaniline					4.08%	0.51%

^a The molecular orbital composition was calculated using the Multiwfn program with Ros-Schuit (SCPA) partition.

To get more information from the frontier orbitals, the composition of the HOMOs and LUMOs has been calculated using the Multiwfn program²⁷. As shown in Table 3, the whole chromophore molecule was segmented as donor, π -bridge, and acceptor. At the same time, the attributions of the steric hindrance groups (methoxyphenyl, N,N-dimethylaniline) located in bridge

moiety were listed separately. For these three chromophores, the LUMO and HOMO were all largely stabilized by the contributions from acceptors and donors. For chromophores CL1 and CL2, when comparing LUMO to HOMO level, the contribution of methoxyphenyl ring decreased to 0.77% from 2.57%, while the N,N-dimethylaniline ring decreased to 0.51% from 4.08%. The

comparison of HOMO and LUMO electron distribution in the methoxyphenyl ring and N,N-dimethylaniline ring indicated the easy delocalization of electrons in these two benzene rings. Consequently, both the methoxyphenyl ring and N,N-dimethylaniline ring can be treated as another donor, which efficiently enhances the electron density of the conjugated system and increases the polarizability of chromophores.

Furthermore, the theoretical microscopic Zero-frequency (static) molecular first hyperpolarizability (β) was calculated using Gaussian 09.²⁶ As a reference reported earlier, β has been calculated at the 6-31+G* level under vacuum²⁸. From this, the scalar quantity of β can be computed from the x, y, and z components according to the following equation²⁹:

$$\beta = (\beta_x^2 + \beta_y^2 + \beta_z^2)^{1/2} \quad (1)$$

Where

$$\beta_i = \beta_{iii} + \frac{1}{3} \sum_{i \neq j} (\beta_{ijj} + \beta_{jij} + \beta_{jji}), i, j \in (x, y, z) \quad (2)$$

When used carefully and consistently, this method of DFT has been shown to give relatively consistent descriptions of first-order hyperpolarizability for a number of similar chromophores.^{30,31}

As reported earlier, the β value has a close relationship with the substituents, steric hindrance, and intramolecular charge-transfer, π -conjugation length and so on.^{32,33} The β values of chromophores CL1 and CL2 were little smaller than that of chromophore CL. This may be explained by that both chromophore CL1 and CL2 possessed a less coplanar geometry due to the steric hindrance of the lateral group methoxyphenyl and N,N-dimethylaniline. Besides, the β value may have much to do with the environmental effect, and this work will be carried out in our group.³⁴

Electrochemical properties

In order to determine the redox properties of chromophores CL, CL1 and CL2, cyclic voltammetry (CV) measurements were conducted in degassed anhydrous acetonitrile solutions containing 0.1 mol/L tetrabutylammonium hexafluorophosphate (TBAPF) as the supporting electrolyte. The relative data and voltammograms of 1×10^{-4} mol/L chromophores CL, CL1 and CL2 were recorded, as shown in Table 2 and Fig. 4.

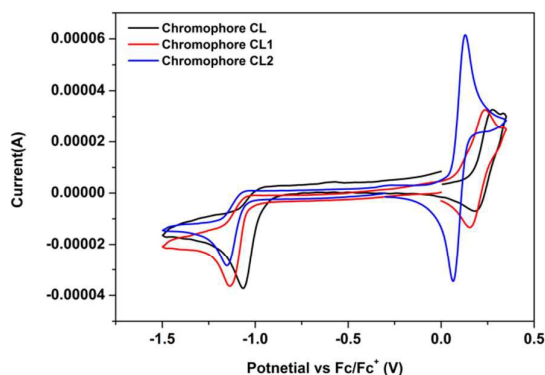


Fig. 4 Cyclic voltammograms of chromophores CL, CL1 and CL2 recorded in CH_3CN solutions containing 0.1 M Bu_4NPF_6 supporting electrolyte at a scan rate of 50 mV s^{-1}

As shown in Fig. 4, chromophores CL, CL1 and CL2 all exhibited one quasi reversible oxidative wave with a half-wave potential, $E_{1/2} = 0.5(E_{\text{ox}} + E_{\text{red}})$, at about 0.23, 0.19 and 0.10 V respectively. Meanwhile, these chromophores had an irreversible reduction wave corresponding to the acceptor moieties at $E_{\text{red}} = -1.06, -1.14$ and -1.15 V (vs. ferrocene/ferrocenium). It showed energy gap (DE) values of 1.29, 1.33 and 1.25 eV for chromophores CL, CL1 and CL2 respectively. The HOMO and LUMO levels of these new chromophores were calculated from their corresponding oxidation and reduction potentials. The HOMO levels of chromophores CL, CL1 and CL2 were estimated to be $-5.03, -4.99$ and -4.90 eV respectively. In the meantime, the corresponding LUMO level of chromophores CL, CL1 and CL2 were estimated to be $-3.74, -3.66$ and -3.65 eV, respectively. These results showed the same trend as the DFT results.

Electro-Optic performance

In order to evaluate the poling efficiency and EO activity of these chromophores, amorphous polycarbonate (APC) guest–host polymer films incorporating these chromophores were prepared, corona poled, and analysed via simple reflection method (Teng-Man) at 1310 nm^{35} , using the corrected formula³⁸. In order to minimize the contribution from multiple reflections, a carefully selected thin ITO electrode with low reflectivity and good transparency was used. The measured r_{33} values depend on the chromophore number density (N), hyperpolarizability (β), and poling efficiency, described by the $\langle \cos^3 \theta \rangle$ order parameter, as indicated by

$$r_{33} = \left| 2Nf(\omega)\beta \langle \cos^3 \theta \rangle / n^4 \right| \quad (3)$$

where n is the refractive index of the film and the $f(\omega)$ term describes electric-field (Debye-Onsager) factors, both of which remain relatively constant for related chromophores at similar loading densities. In order to facilitate meaningful analysis, the loading densities of the guest–host films are presented in terms of N, assuming the overall density of the films remains that of the APC host, which allows normalization of the observed r_{33} values for the chromophore content. The term $\cos^3(\theta)$ is the acentric order parameter. θ is the angle between the permanent dipole moment of chromophores and the applied electric field. When the concentration of chromophore is low, the electro-optic activity increased with chromophore density, dipole moment and the strength of the electric poling field. However, when the concentrations increased to a certain extent, the N and $\cos^3(\theta)$ are no longer independent factors. Then,

$$\langle \cos^3(\theta) \rangle = (\mu F / 5kT) [1 - L^2(W / kT)] \quad (4)$$

where k is the Boltzmann constant and T is the Kelvin (poling) temperature. $F = [f(0)E_p]$ where E_p is the electric poling field. L is the Langevin function, which is a function of W/kT , the ratio of the intermolecular electrostatic energy (W) to the thermal energy (kT). L is related to electrostatic interactions between molecules.⁹

The relationship described above can be successfully applied to qualitatively predict the important trends involving electro-optic activity. When the intermolecular electrostatic interactions are neglected, the electro-optic coefficient (r_{33}) should increase linearly with chromophore density, dipole moment, first hyperpolarizability and the strength of the electric poling field. But chromophores with

large dipole moments generate an intermolecular static electric field dipole-dipole interaction, which leads to the unfavorable antiparallel packing of chromophores. So the number of truly oriented chromophores (N) is small. In molecular optimization, introducing a huge steric hindrance group to isolate chromophores is the most popular and easy way to attenuate the dipole-dipole interactions of chromophores.¹⁸

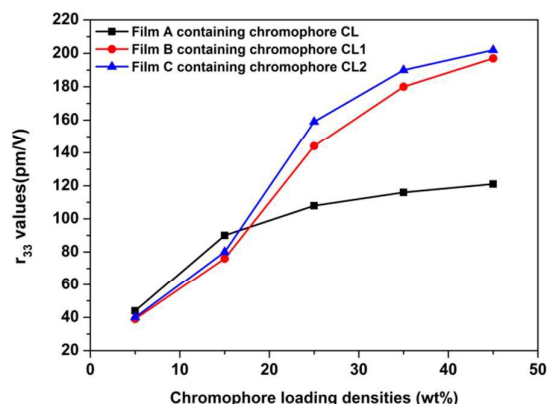


Fig. 5 EO coefficients of NLO thin films as a function of chromophore loading densities

The r_{33} values of films CL/APC, CL1/APC and CL2/APC were measured in different loading densities, as shown in Fig. 5. For chromophore CL, the r_{33} values were gradually improved from 34 pm V^{-1} (5 wt %) to 121 pm V^{-1} (45 wt %). For chromophore CL1, the r_{33} value was improved from 42 pm V^{-1} (5 wt %) to 197 pm V^{-1} (45 wt %), as the concentration of chromophores increased, a similar trend of enhancement was also observed for chromophore CL2, whose r_{33} values increased from 45 pm V^{-1} (5 wt %) to 202 pm V^{-1} (45 wt %). When the concentration of the chromophore in APC is low, film CL/APC displayed a larger r_{33} value than that of films CL1/APC and CL2/APC. As the chromophore loading increased, this trend is reversed. This can be explained by that, when in a low-density range, the intermolecular dipolar interactions are relatively weak. The intermolecular dipole-dipole interactions would become stronger and stronger, accompanied by the increased concentration of NLO chromophore moieties in the polymer which would finally lead to a decreased NLO coefficient. The introduction of steric hindrance groups attached to the conjugated π -system can make inter-chromophore electrostatic interactions less favourable.

The stability of the poled EO films was also investigated. After annealing at 85 °C for 100 h, the poled films of 25%CL/APC, 25%CL1/APC and 25%CL2/APC could retain 78%, 83% and 81% (100 h) of the initial values at 85 °C respectively. This percentage was considerably high enough.

Moreover, the order parameter changes of the poled EO films were studied by recording the UV-Vis absorption spectra of EO films before and after poling. After the corona poling, the chromophores in the polymer were aligned, and the absorption intensity decreased due to birefringence. The order parameter (Φ) can be described according to the following equation: $\Phi = 1 - A_1/A_0$, where A_0 and A_1 are the absorbance of the unpoled and poled EO polymer films at normal incidence. The Φ values of films 25%CL/APC,

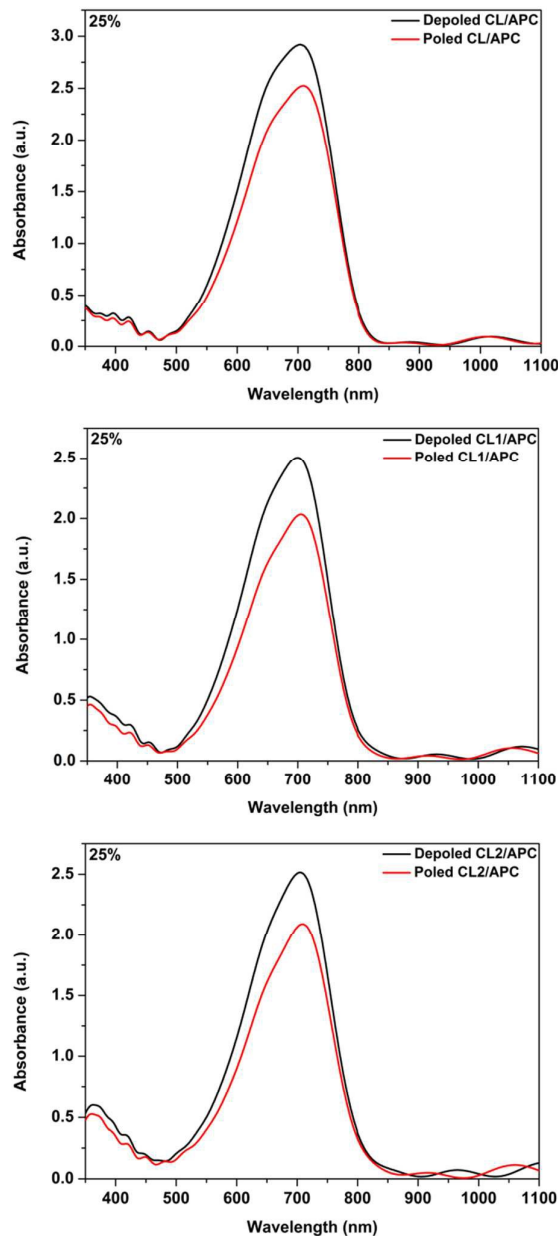


Fig. 6 UV-Vis absorption spectra of EO polymers before and after poling (25 wt %).

25%CL1/APC and 25%CL2/APC were about 13.6%, 18.4% and 17.9% respectively (Fig. 6), which showed that the Φ values had reached the average values and that the poling process was typically efficient. The difference in the order parameter indicates that films CL1/APC and CL2/APC have weaker inter-chromophore electrostatic interactions than film CL/APC in high density. It may be revealed by the optimized configurations (Fig. 7) that the benzene derivative steric hindrance groups were perpendicular to the direction of the dipole moment of the chromophore which could

act as an excellent isolation group to suppress the possible aggregation. The high saturated loading density and larger Φ values of films 25%CL1/APC and 25%CL2/APC were probably attributed to the fact that the chromophore structure isolated the chromophores from each other more effectively, thus improving the NLO effect at a higher chromophore loading density level.⁵

Through the outcome above, we can obviously see that chromophores CL1 and CL2 containing benzene derivative steric hindrance groups on the π -electron bridges have nearly 2 times higher r_{33} values than chromophore CL with no steric hindrance on the π -electron bridge, illustrating that chromophores CL1 and CL2 can translate their relatively low β values into bulk EO activities more effectively than chromophore CL due to the isolation of benzene derivative steric hindrance groups on the π -electron bridge. Moreover, the large r_{33} values (5 times of FTC, 39 pm V^{-1})³⁶ of chromophores CL1 and CL2 suggest brilliant broad prospects in advanced material devices.

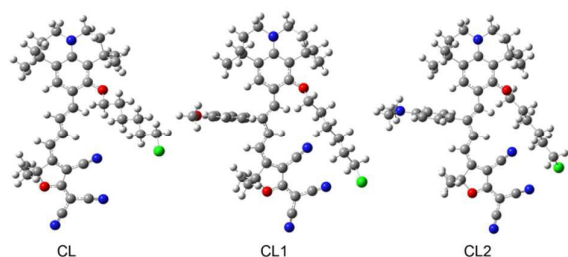


Fig. 7 The optimized structure of chromophores CL, CL1 and CL2.

Experimental

Materials and instrument

All chemicals are commercially available and are used without further purification unless otherwise stated. *N,N*-dimethylformamide (DMF), Phosphorus oxychloride (POCl_3), tetrahydrofuran (THF) and ether were distilled over calcium hydride and stored over molecular sieves (pore size 3\AA). (4-Methoxybenzyl)-triphenylphosphonium Bromide and (4-Dimethylamino)-triphenylphosphonium Bromide were synthesized according to the literature³⁷. 2-Dicyanomethylene-3-cyano-4-methyl-2,5-dihydrofuran (TCF) acceptor was prepared according to the literature³⁸. TLC analyses were carried out on 0.25 mm thick precoated silica plates and spots were visualized under UV light. Chromatography on silica gel was carried out on Kieselgel (200-300 mesh).

Measurements and instrumentation

^1H NMR and ^{13}C NMR spectra were determined on an Advance Bruker 400M (400 MHz) NMR spectrometer (tetramethylsilane as internal reference). The MS spectra were obtained on MALDI-TOF (Matrix Assisted Laser Desorption/Ionization of Flight) on BIFLEXIII (Broker Inc.) spectrometer. The UV-Vis spectra were performed on Cary 5000 photo spectrometer. The TGA was determined by TA5000-2950TGA (TA co) with a heating rate of $10 \text{ }^\circ\text{C min}^{-1}$ under the protection of nitrogen. Cyclic voltammetric data were measured on a Princeton Applied Research Model 283 Potentiostat

/Galvanostat. The DFT calculations using Gaussian 09 were carried out at the hybrid B3LYP level by employing the split valence 6-31G* basis set.³⁰

Syntheses and characterization

Compound 2

A two-phase mixture of 8-hydroxy-1,1,7,7-tetramethyljulolidine-9-carboxaldehyde (5.47g, 20 mmol), 1,6-dichlorohexane (30 mL), tetrabutyl ammonium bromide (0.3 g, 1 mmol), and 1M NaOH (30mL) was heated to reflux for 6 h. The mixture was diluted with ether (50 mL) and washed with HCl (1 M, 15 mL) and water (2×25 mL). The combined organic extracts were dried over MgSO_4 . After removal of the solvent under reduced pressure, the residue was purified by column chromatography (hexane /acetone, 20/1, v/v) to give a yellowish oils **2** (7.29g, 18.6mmol) liquid in 93.0% yield.

MS(MALDI-TOF): m/z (M^+ , $\text{C}_{23}\text{H}_{34}\text{ClNO}_2$): calcd:391.23; found: 391.226.

^1H NMR (400 MHz, CDCl_3) δ 9.92 (s, 1H), 7.59 (s, 1H), 3.96 (t, $J = 6.8$ Hz, 2H), 3.56 (t, $J = 6.7$ Hz, 2H), 3.33 – 3.28 (m, 2H), 3.26 – 3.21 (m, 2H), 1.94 – 1.87 (m, 2H), 1.86 – 1.79 (m, 2H), 1.77 – 1.70 (m, 4H), 1.53 (dt, $J = 7.1, 3.4$ Hz, 4H), 1.43 (s, 6H), 1.27 (s, 6H).

Compound 4a

To a solution of **1** (0.55 g, 1.5 mmol) and tributyl(1,3-dioxolan-2-ylmethyl)phosphonium bromide (**3a**) (1.2 g, 3.3 mmol) in anhydrous THF was added a sodium hydride (0.1g, 4.5 mmol), 18-crown-6 as the catalyst. After the mixture was stirred at room temperature for 20 h, HCl/THF (v/v) solution was added to quenching the reaction and kept to stir for another 1 h. Then, the organic layers were extracted with ethyl acetate (3×50 ml). The combined organic extracts were dried over MgSO_4 . After the removal of the solvent, the residue was purified by column chromatography (hexane /acetone, 15/1, v/v) to give a yellow oils **4a** (0.38 g, 0.95 mmol) in 63.5% yield.

MS(MALDI-TOF): m/z (M^+ , $\text{C}_{23}\text{H}_{34}\text{ClNO}_2$): calcd:417.24; found: 417.238.

^1H NMR (400 MHz, CDCl_3) δ 9.57 (d, $J = 8.0$ Hz, 1H), 7.61 (s, 0.5H), 7.57 (s, 0.5H), 7.32 (s, 1H), 6.53 (dd, $J = 15.6, 8.0$ Hz, 1H), 3.82 (t, $J = 6.8$ Hz, 2H), 3.56 (t, $J = 6.6$ Hz, 2H), 3.29 – 3.24 (m, 2H), 3.22 – 3.17 (m, 2H), 1.89 (dd, $J = 11.8, 4.9$ Hz, 2H), 1.86 – 1.80 (m, 2H), 1.72 (dd, $J = 11.5, 4.6$ Hz, 4H), 1.55 (dt, $J = 7.1, 3.5$ Hz, 4H), 1.41 (s, 6H), 1.26 (s, 6H).

Chromophore CL

A solution of **4a** (0.15 g, 0.38 mmol) and TCF (0.06 g, 0.45 mmol) in 50 ml ethanol was refluxed under microwaves for 2 h, then cooled to room temperature. After the removal of the solvent, the residue was purified by column chromatography (hexane / AcOEt, 3/1, v/v) to give a green solid chromophore CL (0.17 g, 0.28 mmol) in 73% yield.

MS(MALDI-TOF): m/z (M^+ , $\text{C}_{36}\text{H}_{43}\text{ClN}_4\text{O}_2$): calcd:598.31; found: 598.321.

^1H NMR (400 MHz, CDCl_3) δ 7.81 – 7.65 (m, 1H), 7.34 (d, $J = 16.0$ Hz, 2H), 6.87 (dd, $J = 14.6, 11.5$ Hz, 1H), 6.29 (d, $J = 14.8$ Hz, 1H), 3.83 (t, $J = 6.7$ Hz, 2H), 3.58 (t, $J = 6.6$ Hz, 2H), 3.38 (t, $J = 6.0$ Hz, 2H), 3.34 – 3.26 (m, 2H), 1.96 – 1.88 (m, 2H), 1.83 (dd, $J = 13.3, 6.6$ Hz, 2H), 1.77 – 1.72 (m, 4H), 1.69 (s, 6H), 1.61 – 1.53 (m, 4H), 1.42 (s, 6H), 1.30 (s,

6H). ^{13}C NMR (101 MHz, CDCl_3) δ 176.65, 172.95, 159.57, 151.12, 147.53, 145.86, 127.67, 124.51, 122.46, 122.11, 116.67, 113.29, 112.87, 112.46, 112.27, 96.43, 91.70, 77.33, 76.71, 53.13, 47.77, 47.14, 45.12, 39.11, 35.39, 32.54, 32.44, 32.11, 30.03, 29.90, 29.70, 29.56, 26.75, 26.64, 25.45, 19.18.

Compound 4b

Under a N_2 atmosphere, to a solution of **2** (3.92g, 10mmol) and **3b** (5.10 g, 11 mmol) in dry THF (40 mL) was added NaH (2.40 g, 0.10mol). The solution was allowed to stir for 24 h at room temperature and then poured into ice water. The organic phase was extracted using ethyl acetate, washed with brine and dried over MgSO_4 . After removal of the solvent under reduced pressure, the residue was purified by column chromatography (hexane /acetone, 30/1, v/v) to give a yellowish solid **4b** (4.17 g, 8.43 mmol) in 84.3% yield. The ratio of the Z : E isomer is 60 : 40% calculated by the integration of respective protons.

MS(MALDI-TOF): m/z (M^+ , $\text{C}_{31}\text{H}_{42}\text{ClNO}_2$): calcd: 495.29; found: 495.307.

^1H NMR (400 MHz, CDCl_3) δ 7.40 (d, J = 8.6 Hz, 0.8H), 7.31 (d, J = 8.7 Hz, 1.2H), 7.26 (s, 0.4H), 7.08 (d, J = 16.3 Hz, 0.4H), 6.98 (s, 0.6H), 6.87 (d, J = 8.6 Hz, 0.8H), 6.78 (d, J = 16.3 Hz, 0.4H), 6.74 (d, J = 8.7 Hz, 1.2H), 6.43 (d, J = 12.0 Hz, 0.6H), 6.32 (d, J = 12.1 Hz, 0.6H), 3.97 (t, J = 6.6 Hz, 1.2H), 3.85 (t, J = 6.6 Hz, 0.8H), 3.79 (s, 1.2H), 3.74 (s, 1.8H), 3.49 (dt, J = 13.5, 6.7 Hz, 2H), 3.15 – 3.08 (m, 0.8H), 3.03 (dt, J = 11.0, 5.3 Hz, 3.2H), 1.87 – 1.70 (m, 6.8H), 1.69 – 1.62 (m, 1.2H), 1.55 – 1.45 (m, 4H), 1.42 (s, 2.4H), 1.41 (s, 3.6H), 1.30 (s, 2.4H), 1.01 (s, 3.6H).

Compound 5b

A solution of 10 ml DMF was cooled to 0 °C and was maintained at this temperature during the dropwise addition of phosphorus oxychloride (0.92 g, 6 mmol). The solution was kept for 2 h of stirring at 0°C and the temperature was kept during the dropwise addition of compound **4b** in 30 ml DMF (1.99 g, 4 mmol). The solution was gradually warmed to room temperature and stirred for 2 h of stirring at 60°C before being poured into 200 ml solution of sodium carbonate (10%) for quench. The reaction mixture was extracted by ethyl acetate, washed with brine, dried over MgSO_4 . After removal of the solvent under reduced pressure, the residue was purified by column chromatography (hexane /acetone, 15/1, v/v) to give a yellow solid **5b** (1.82 g, 3.48 mmol) in 86.9% yield.

MS(MALDI-TOF): m/z (M^+ , $\text{C}_{32}\text{H}_{42}\text{ClNO}_3$): calcd:524.14; found: 524.291.

^1H NMR (400 MHz, CDCl_3) δ 9.65 (s, 1H), 7.48 (s, 1H), 7.20 (d, J = 8.1 Hz, 2H), 6.96 (d, J = 8.1 Hz, 2H), 6.77 (s, 1H), 3.95 (t, J = 6.5 Hz, 2H), 3.82 (s, 3H), 3.57 (t, J = 6.6 Hz, 2H), 3.15 (dd, J = 12.4, 7.0 Hz, 4H), 1.92 (dd, J = 14.2, 7.3 Hz, 2H), 1.84 (dd, J = 13.4, 6.7 Hz, 2H), 1.75 – 1.69 (m, 2H), 1.63 – 1.54 (m, 6H), 1.42 (s, 6H), 0.82 (s, 6H).

Chromophore CL1

The procedure for chromophore CL was followed to prepare chromophore CL1 from **5b** as a green solid in 68.9% yield (0.24 g, 0.34 mmol).

MS(MALDI-TOF): m/z (M^+ , $\text{C}_{32}\text{H}_{42}\text{ClNO}_3$): calcd:705.35; found: 705.326.

^1H NMR (400 MHz, CDCl_3) δ 8.04 (d, J = 15.1 Hz, 1H), 7.35 (s, 1H), 7.12 (d, J = 8.6 Hz, 2H), 7.04 (d, J = 8.6 Hz, 2H), 6.53 (s, 1H), 5.82 (d, J = 15.2 Hz, 1H), 3.93 (t, J = 6.6 Hz, 2H), 3.86 (s, 3H), 3.59 (t, J = 6.5 Hz,

2H), 3.26 – 3.17 (m, 4H), 1.98 – 1.92 (m, 2H), 1.90 – 1.83 (m, 2H), 1.82 – 1.76 (m, 2H), 1.68 – 1.59 (m, 6H), 1.58 (s, 6H), 1.41 (s, 6H), 0.81 (s, 6H). ^{13}C NMR (101 MHz, CDCl_3) δ 176.76, 173.07, 160.21, 159.55, 154.94, 146.55, 144.79, 134.88, 130.92, 130.67, 128.85, 128.75, 127.33, 126.33, 121.94, 116.22, 115.39, 113.15, 112.23, 112.14, 110.99, 96.49, 91.75, 77.25, 77.10, 55.44, 53.57, 47.58, 46.97, 45.14, 39.29, 35.45, 32.50, 32.44, 31.64, 29.99, 29.70, 29.67, 29.63, 26.80, 26.39, 25.60, 19.17.

Compound 4c

The procedure for compound **4b** was followed to prepare **4c** from **2** and **3c** as a yellowish oil in 73.1% yield (3.72 g, 7.31 mmol). The ratio of the Z : E isomer is 50 : 50% calculated by the integration of respective protons.

MS(MALDI-TOF): m/z (M^+ , $\text{C}_{32}\text{H}_{42}\text{ClNO}_3$): calcd:508.33; found: 508.256.

^1H NMR (400 MHz, Acetone) δ 7.27 – 7.20 (m, 1.33H), 7.10 (d, J = 5.7 Hz, 1H), 6.95 – 6.82 (m, 1.2H), 6.73 (d, J = 10.5 Hz, 0.37H), 6.61 (d, J = 8.7 Hz, 1H), 6.52 (d, J = 8.4 Hz, 0.15H), 6.47 (d, J = 8.8 Hz, 1H), 6.17 (s, 1H), 3.88 (t, J = 6.6 Hz, 1H), 3.72 (t, J = 6.5 Hz, 1H), 3.45 (q, J = 6.6 Hz, 2H), 3.10 – 2.87 (m, 4H), 2.82 (s, 3H), 2.76 (s, 3H), 1.79 – 1.63 (m, 4H), 1.63 – 1.51 (m, 4H), 1.50 – 1.33 (m, 4H), 1.30 – 1.26 (m, 6H), 1.15 (s, 3H), 0.90 (s, 3H).

Compound 5c

The procedure for compound **5b** was followed to prepare **5c** from **4c** as a yellow solid in 83.3% yield (1.79 g, 3.33 mmol).

MS(MALDI-TOF): m/z (M^+ , $\text{C}_{33}\text{H}_{45}\text{ClN}_2\text{O}_2$): calcd:536.32; found: 536.239.

^1H NMR (400 MHz, CDCl_3) δ 9.65 (s, 1H), 7.43 (s, 1H), 7.14 (d, J = 8.3 Hz, 2H), 6.85 (s, 1H), 6.79 (d, J = 7.2 Hz, 2H), 3.96 (t, J = 6.6 Hz, 2H), 3.57 (t, J = 6.6 Hz, 2H), 3.19 – 3.07 (m, 4H), 2.93 (s, 6H), 1.95 – 1.89 (m, 2H), 1.84 (m, 2H), 1.74 – 1.68 (m, 2H), 1.62 – 1.53 (m, 6H), 1.41 (s, 6H), 0.83 (s, 6H).

Chromophore CL2

The procedure for chromophore CL was followed to prepare chromophore CL2 from **5c** as a green solid in 70.2% yield (0.31 g, 0.43 mmol).

MS(MALDI-TOF): m/z (M^+ , $\text{C}_{33}\text{H}_{45}\text{ClN}_2\text{O}_2$): calcd:718.36; found: 718.382.

^1H NMR (400 MHz, CDCl_3) δ 8.06 (d, J = 15.0 Hz, 1H), 7.36 (s, 1H), 7.04 (d, J = 8.3 Hz, 2H), 6.86 (s, 2H), 6.58 (s, 1H), 5.88 (d, J = 15.0 Hz, 1H), 3.92 (t, J = 6.5 Hz, 2H), 3.59 (t, J = 6.6 Hz, 2H), 3.21 (dd, J = 13.5, 7.5 Hz, 4H), 3.01 (s, 6H), 1.93 – 1.85 (m, 2H), 1.85 – 1.83 (s, 2H), 1.71 – 1.67 (m, 2H), 1.62 – 1.55 (m, 12H), 1.39 (s, 6H), 0.80 (s, 6H).

^{13}C NMR (101 MHz, CDCl_3) δ 176.87, 173.15, 160.16, 159.38, 155.41, 146.46, 144.96, 135.85, 130.27, 130.13, 128.93, 128.86, 127.50, 126.21, 121.80, 116.55, 113.93, 113.28, 112.34, 112.25, 111.11, 96.48, 91.36, 77.25, 77.11, 60.39, 53.26, 47.56, 46.97, 45.14, 40.69, 39.37, 35.59, 32.49, 32.45, 31.65, 30.00, 29.78, 29.70, 29.69, 26.81, 26.41, 25.60, 19.17.

Conclusions

In this article, three NLO chromophores CL, CL1 and CL2 based on modified 8-hydroxy-1, 1, 7, 7-tetramethyl-formyljulolidine as the donor and tricyanofuran (TCF) as the acceptor had been synthesized in good overall yields (40%~50%) and systematically

characterized by NMR, MS and UV-Vis absorption spectroscopy. Chromophores CL1 and CL2 had been synthesized with different additional steric hindrance groups (methoxyphenyl and N,N-dimethylaniline) on the π -electron bridge. Chromophore CL was chosen as a reference compound for comparison. Thermal stability was studied, and the results indicated that after introducing benzene derivative steric hindrance groups into the bridge, chromophores CL1 and CL2 showed good thermal stabilities with quite high thermal decomposition temperatures 273 °C and 265 °C, respectively. The energy gaps between the ground state and the excited state together with molecular nonlinearity were studied by UV-Vis absorption spectroscopy, DFT calculations and CV measurements. Theoretical and experimental investigations suggested that the steric hindrance group played a critical role in affecting the linear and nonlinear properties of dipolar chromophores. The poling results of guest–host EO polymers with 45 wt % of chromophores showed that polymers with chromophores CL1 and CL2 afforded the largest r_{33} values of 197, and 202 pm V⁻¹ respectively, which were about 1.6 times of chromophore CL (just 121 pm V⁻¹). However, polymers with chromophore CL afforded the largest r_{33} value just 121 pm V⁻¹. These consequences indicated that chromophores with benzene derivative steric hindrance groups on the π -electron bridges could efficiently reduce dipole–dipole interactions so as to translate their relatively small β values into bulk EO performance more effectively. These novel chromophores accompanied with advantages of high-yield synthesis, excellent thermal stability and considerably high nonlinear optical activity showed brilliant broad application prospects in organic EO and photorefractive materials area.

Acknowledgements

We are grateful to the National Natural Science Foundation of China (No. 21504099 and No. 21003143) for the financial support. All calculations were performed on the cluster of Key Laboratory of Theoretical and Computational Photochemistry, Ministry of Education, China.

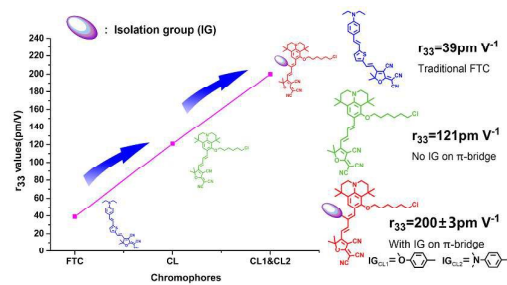
Notes and references

- O. Ostroverkhova and W. E. Moerner, *Chemical Reviews*, 2004, 104, 3267-3314.
- X. M. Zheng, A. Sinyukov and L. M. Hayden, *Applied Physics Letters*, 2005, 87.
- Q. F. Xu, B. Schmidt, S. Pradhan and M. Lipson, *Nature*, 2005, 435, 325-327.
- T. Baehr-Jones, M. Hochberg, G. X. Wang, R. Lawson, Y. Liao, P. A. Sullivan, L. Dalton, A. K. Y. Jen and A. Scherer, *Optics Express*, 2005, 13, 5216-5226.
- Y. H. Kuo, J. D. Luo, W. H. Steier and A. K. Y. Jen, *Ieee Photonics Technology Letters*, 2006, 18, 175-177.
- S. K. Kim, Y. C. Hung, B. J. Seo, K. Geary, W. Yuan, B. Bortnik, H. R. Fetterman, C. Wang, W. H. Steier and C. Zhang, *Applied Physics Letters*, 2005, 87.
- Y. Yang, H. Wang, F. Liu, D. Yang, S. Bo, L. Qiu, Z. Zhen and X. Liu, *Physical Chemistry Chemical Physics*, 2015, 17, 5776-5784.
- S. R. Hammond, O. Clot, K. A. Firestone, D. H. Bale, D. Lao, M. Haller, G. D. Phelan, B. Carlson, A. K. Y. Jen, P. J. Reid and L. R. Dalton, *Chemistry of Materials*, 2008, 20, 3425-3434.
- F. Liu, H. Wang, Y. Yang, H. Xu, M. Zhang, A. Zhang, S. Bo, Z. Zhen, X. Liu and L. Qiu, *Journal of Materials Chemistry C*, 2014, 2, 7785-7795.
- F. Dumur, C. R. Mayer, E. Dumas, F. Miomandre, M. Frigoli and F. Secheresse, *Organic Letters*, 2008, 10, 321-324.
- R. M. El-Shishtawy, F. Borbone, Z. M. Al-Amshany, A. Tuzi, A. Barsella, A. M. Asiri and A. Roviello, *Dyes and Pigments*, 2013, 96, 45-51.
- H. Wang, F. Liu, Y. Yang, H. Xu, C. Peng, S. Bo, Z. Zhen, X. Liu and L. Qiu, *Dyes and Pigments*, 2015, 112, 42-49.
- Y. Yang, J. Liu, M. Zhang, F. Liu, H. Wang, S. Bo, Z. Zhen, L. Qiu and X. Liu, *Journal of Materials Chemistry C*, 2015, 3, 3913-3921.
- J. Liu, A. V. Franiv, X. Liu and Z. Zhen, *Journal of Materials Science-Materials in Electronics*, 2013, 24, 2701-2705.
- I. V. Kosilkin, E. A. Hillenbrand, P. Tongwa, A. Fonari, J. Zazueta, M. S. Fonari, M. Antipin, L. R. Dalton and T. Timofeeva, *Journal of Molecular Structure*, 2011, 1006, 356-365.
- H. Huang, J. Liu, Z. Zhen, L. Qiu, X. Liu, G. Lakshminarayana, S. Tkaczyk and I. V. Kityk, *Materials Letters*, 2012, 75, 233-235.
- P. Si, J. Liu, G. Deng, H. Huang, H. Xu, S. Bo, L. Qiu, Z. Zhen and X. Liu, *Rsc Advances*, 2014, 4, 25532-25539.
- J. Wu, C. Peng, H. Xiao, S. Bo, L. Qiu, Z. Zhen and X. Liu, *Dyes and Pigments*, 2014, 104, 15-23.
- P. Si, J. L. Liu, G. W. Deng, H. Y. Huang, H. J. Xu, S. H. Bo, L. Qiu, Z. Zhen and X. H. Liu, *Rsc Advances*, 2014, 4, 25532-25539.
- J. Liu, G. Xu, F. Liu, I. Kityk, X. Liao and Z. Zhen, *Rsc Advances*, 2015, 5, 15784-15794.
- J. Wu, H. Xiao, L. Qiu, Z. Zhen, X. Liu and S. Bo, *Rsc Advances*, 2014, 4, 49737-49744.
- K. Tang, M. Liang, Y. Liu, Z. Sun and S. Xue, *Chinese Journal of Chemistry*, 2011, 29, 89-96.
- T. Kitamura, M. Ikeda, K. Shigaki, T. Inoue, N. A. Anderson, X. Ai, T. Q. Lian and S. Yanagida, *Chemistry of Materials*, 2004, 16, 1806-1812.
- C. Zhang, L. R. Dalton, M. C. Oh, H. Zhang and W. H. Steier, *Chemistry of Materials*, 2001, 13, 3043-3050.
- X. Piao, X. Zhang, S. Inoue, S. Yokoyama, I. Aoki, H. Miki, A. Otomo and H. Tazawa, *Organic Electronics*, 2011, 12, 1093-1097.
- M. J. Frisch, G. W. Trucks, H. B. Schlegel, G. E. Scuseria, M. A. Robb, J. R. Cheeseman, J. A. Montgomery, Jr., T. Vreven, K. Kudin, J. C. Burant and e. al., *Gaussian 09, revision A.02*, Gaussian, Inc: Wallingford CT, 2009.
- R. V. Solomon, P. Veerapandian, S. A. Vedha and P. Venuvanalingam, *Journal of Physical Chemistry A*, 2012, 116, 4667-4677.
- A. Zhang, H. Xiao, S. Cong, M. Zhang, H. Zhang, S. Bo, Q. Wang, Z. Zhen and X. Liu, *Journal of Materials Chemistry C*, 2015, 3, 370-381.
- K. S. Thanthiriatte and K. M. N. de Silva, *Journal of Molecular Structure-Theochem*, 2002, 617, 169-175.
- X.-H. Zhou, J. Davies, S. Huang, J. Luo, Z. Shi, B. Polishak, Y.-J. Cheng, T.-D. Kim, L. Johnson and A. Jen, *Journal of Materials Chemistry*, 2011, 21, 4437-4444.

ARTICLE

Journal Name

31. C. M. Isborn, A. Leclercq, F. D. Vila, L. R. Dalton, J. L. Bredas, B. E. Eichinger and B. H. Robinson, *Journal of Physical Chemistry A*, 2007, 111, 1319-1327.
32. L. T. Cheng, W. Tam, S. R. Marder, A. E. Stiegman, G. Rikken and C. W. Spangler, *Journal of Physical Chemistry*, 1991, 95, 10643-10652.
33. L. T. Cheng, W. Tam, S. H. Stevenson, G. R. Meredith, G. Rikken and S. R. Marder, *Journal of Physical Chemistry*, 1991, 95, 10631-10643.
34. J. Kulhanek, F. Bures, A. Wojciechowski, M. Makowska-Janusik, E. Gondek and I. V. Kityk, *Journal of Physical Chemistry A*, 2010, 114, 9440-9446.
35. C. C. Teng and H. T. Man, *Applied Physics Letters*, 1990, 56, 1734-1736.
36. Y. Yang, H. Xu, F. Liu, H. Wang, G. Deng, P. Si, H. Huang, S. Bo, J. Liu, L. Qiu, Z. Zhen and X. Liu, *Journal of Materials Chemistry C*, 2014, 2, 5124-5132.
37. E. Longhi, A. Bossi, G. Di Carlo, S. Maiorana, F. De Angelis, P. Salvatori, A. Petrozza, M. Binda, V. Roviati, P. R. Mussini, C. Baldoli and E. Licandro, *European Journal of Organic Chemistry*, 2013, DOI: 10.1002/ejoc.201200958, 84-94.
38. M. Q. He, T. M. Leslie and J. A. Sinicropi, *Chemistry of Materials*, 2002, 14, 2393-2400.



Introducing benzene derivative isolation group into π -bridge improved the EO coefficient (r_{33}) greatly